Revista Brasileira de Paleontologia, 25(4):274–291, Outubro/Dezembro 2022
A Journal of the Brazilian Society of Paleontology

doi:10.4072/rbp.2022.4.03

NEW AGGLUTINATED FORAMINIFERA FROM EARLY EOCENE DEPOSITS OF MAHALLAT REGION, CENTRAL IRAN: IMPLICATION ON BIOSTRATIGRAPHY AND PALEOECOLOGY

SEYED AHMAD BABAZADEH
Department of Sciences, Payame Noor University, Po. Box 19395-3697, Tehran, Iran.
sababazadeh@pnu.ac.ir, *seyedbabazadeh@yahoo.com*

ABSTRACT – This paper describes the foraminiferal associations along with the presentation of three new agglutinated conical foraminiferal species to the construction of the biozonation framework in the Mahallat region of central Iran. The stratigraphic distribution of benthic foraminifers is used to characterize three assemblage zones that are in ascending order: rotaliids-valvulinids Assemblage Zone, alveolinids-coskinolinids Assemblage Zone, and nummulitids-discocyclinids Assemblage Zone. These associations are characterized by marker fossils and localized from the inner ramp to the proximal outer ramp depositional environments. Their biostratigraphic range is assigned to the middle Cuisian to early Lutetian. In addition, three new agglutinated conical foraminiferal species: *Daviesiconus mahallatensis* sp. nov., *Barattolites arghadehensis* sp. nov., and *Coleiconus minimus* sp. nov. are described and figured for the first time from the lower Eocene shallow-water limestone in the studied area. These new species have common characteristics such as eccentric conical test with a low number of comparably coiled chambers in the early stage and uniserial chambers in the adult stage, but they differ in size, the form of test, and radial subepidermal partitions (beams, intercalary beams, and rafters). They are associated with the index *Alveolina* fauna and their biostratigraphic range is assigned to middle–late Cuisian (Ypresian, Early Eocene).

Keywords: biostratigraphy, Early Eocene, new taxa, Mahallat, Iran.

RESUMO – Este trabalho descreve as associações de foraminíferos juntamente com a apresentação de três novas espécies de foraminíferos aglutinantes cônicos, visando a elaboração do arcabouço bioestratigráfico na região de Mahallat, no Irã Central. A distribuição estratigráfica dos foraminíferos bentônicos é utilizada para caracterizar três zonas de associação, da base para o topo: Zona de Associação Rotalídeos–Valvulinídeos, Zona de Associação Alveolinídeos–Coskinolinídeos, e Zona de Associação Numulitídeos–Discoclinídeos. Estas associações são caracterizadas por fósseis marcadores e localizadas desde a plataforma interna até aos ambientes de deposição em plataforma externa proximal. O intervalo bioestratigráfico é atribuído do Cuisiano médio ao início do Luteciano. Além disso, três novas espécies de foraminíferos aglutinantes cônicos, *Daviesiconus mahallatensis* sp. nov., *Barattolites arghadehensis* sp. nov. e *Coleiconus minimus* sp. nov., são descritas e figuradas pela primeira vez em amostras do calcário de águas rasas do Eoceno Inferior na área estudada. Essas novas espécies apresentam características em comum, tais como a testa cônica excêntrica, baixo número de câmaras enroladas no estágio inicial e câmaras unisseriais no estágio adulto, mas diferem em tamanho, formato da testa e divisórias subepidérmicas radiais ("beams, intercalary beams, and rafters"). Elas estão associadas à fauna-índice *Alveolina* e sua distribuição biostratigráfica é atribuído ao Cuisiano médio–superior (Ypresiano, Eoceno Inferior).

Palavras-chave: bioestratigrafia, Eoceno Inferior, espécies novas, Mahallat, Irã.

INTRODUCTION

The studied area (Mahallat region) is geographically located at the border of the Sanandaj-Sirjan zone and Central Iran. Due to structural complexity, it is very difficult to precisely determine the boundary between these two structural zones. It seems to belong to the Sanandaj-Sirjan zone (northeast Esfahan-Sirjan Block). There is no clear lateral continuity due to fault-controlled sedimentological changes (Figure 1).

The larger benthic foraminifers are important shallow-water fauna from the Eocene deposits of the studied area in Central Iran. They are marker fossils used for the reconstruction of the paleo-environment and high-resolution biostratigraphy in various shallow marine deposits of the tropical and subtropical regions (Hottinger, 1960, 2007; Schaub, 1966, 1973, 1981; Rahaghi & Schaub, 1976; Drobne, 1977; Rahaghi, 1980, 1983; Racey, 1994; Serra-Kiel *et al*., 1998; Scheibner *et al*., 2005, 2007; Babazadeh, 2008; Scheibner & Speijer, 2008; Zamagni *et al*., 2008; Afzal *et al*., 2011; Drobne *et al*., 2011; Zhang *et al*., 2013; Nafarieh *et al*., 2019).

All of the recorded benthic foraminiferal specimens could be subdivided into three groups based on the composition and morphology of the test. They include agglutinated, porcellaneous, and hyaline foraminiferal tests, among which only the agglutinated foraminifers are the target of this paper. The Paleogene agglutinated conical foraminifera along

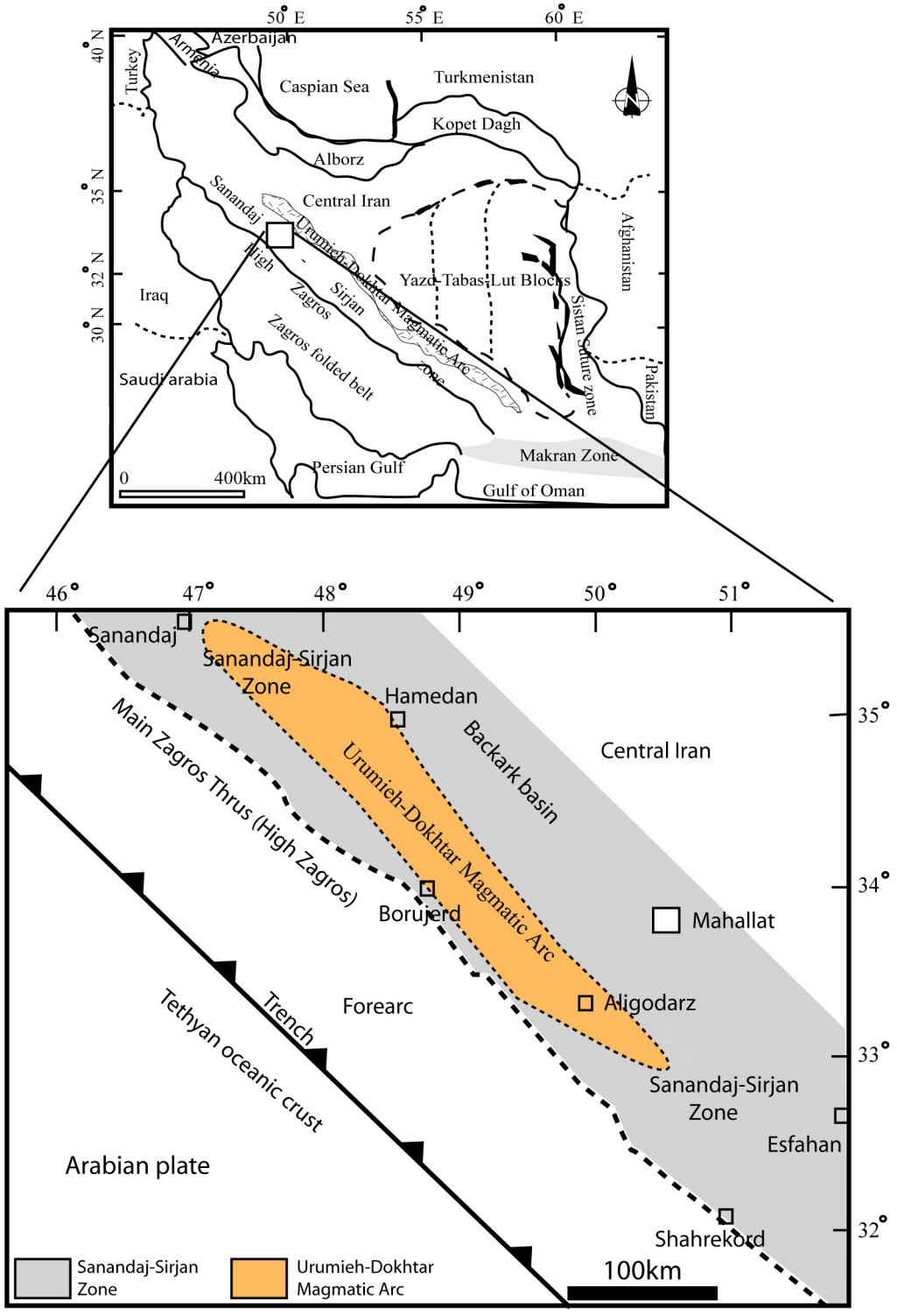

Figure 1. Iran map showing the tectonostratigraphic zones from west/south parts of Iran (Zagros Zone, Sanandaj-Sirjan Zone, Urumieh-Dokhtar Magmatic Arc, Central Iran) and study area (Mahallat region).

with orbitolinids, alveolinids, miliolids, and nummulitids occupied a wide range of shallow water environments. Due to the presence of small miliolids, the agglutinated conical foraminifers indicate a shelf environment with restricted circulation. The agglutinated conical foraminifera are rarely preserved in shallow water facies for this reason they were poorly identified (Hottinger & Drobne, 1980; Hottinger, 2007).

The three genera *Daviesiconus* Hottinger & Drobne (type species: *Coskinolina balsilliei* Davies), *Coleiconus* Hottinger & Drobne (type species: *Coskinolina elongata* Cole), and *Barattolites* Vecchio & Hottinger, were first

reported by Davies (1930), Cole (1942), and Vecchio (2003), respectively. Hottinger & Drobne (1980) carefully studied the internal structure of *Daviesiconus* and *Coleiconus*. The exoskeleton of agglutinated conical foraminifera with simple radial partitions (beams and intercalary beams) was described in detail by Vecchio & Hottinger (2007) for *Barattolites trentinarensis* Vecchio & Hottinger in the Trentinara Formation of Southern Italy. Similar specimens with *B. trentinarensis* were observed in Iranian material from south Iran (Zagros Mountain) (Hottinger, 2007). Several taxa of conical agglutinated foraminifera from the Mahalat Region of central Iran are defined in this article. Among them, three new taxa: *Daviesiconus mahallatensis* sp. nov., *Coleiconus minimus* sp. nov. and *Barattolites arghadehensis* sp. nov. are established for the first time. These new species are recorded from the Eocene carbonate deposits of the study area.

MATERIAL AND METHODS

The paleontological study of larger benthic foraminifera was based on optical microscopy analysis of specimens from 121 thin sections of carbonate rocks. The study section, about 400 m thick, is well exposed in the quadrangle defined by 33°46'00'', 33°46'15''N and 50°25'00'', 50°25'10''E (Figure 2).

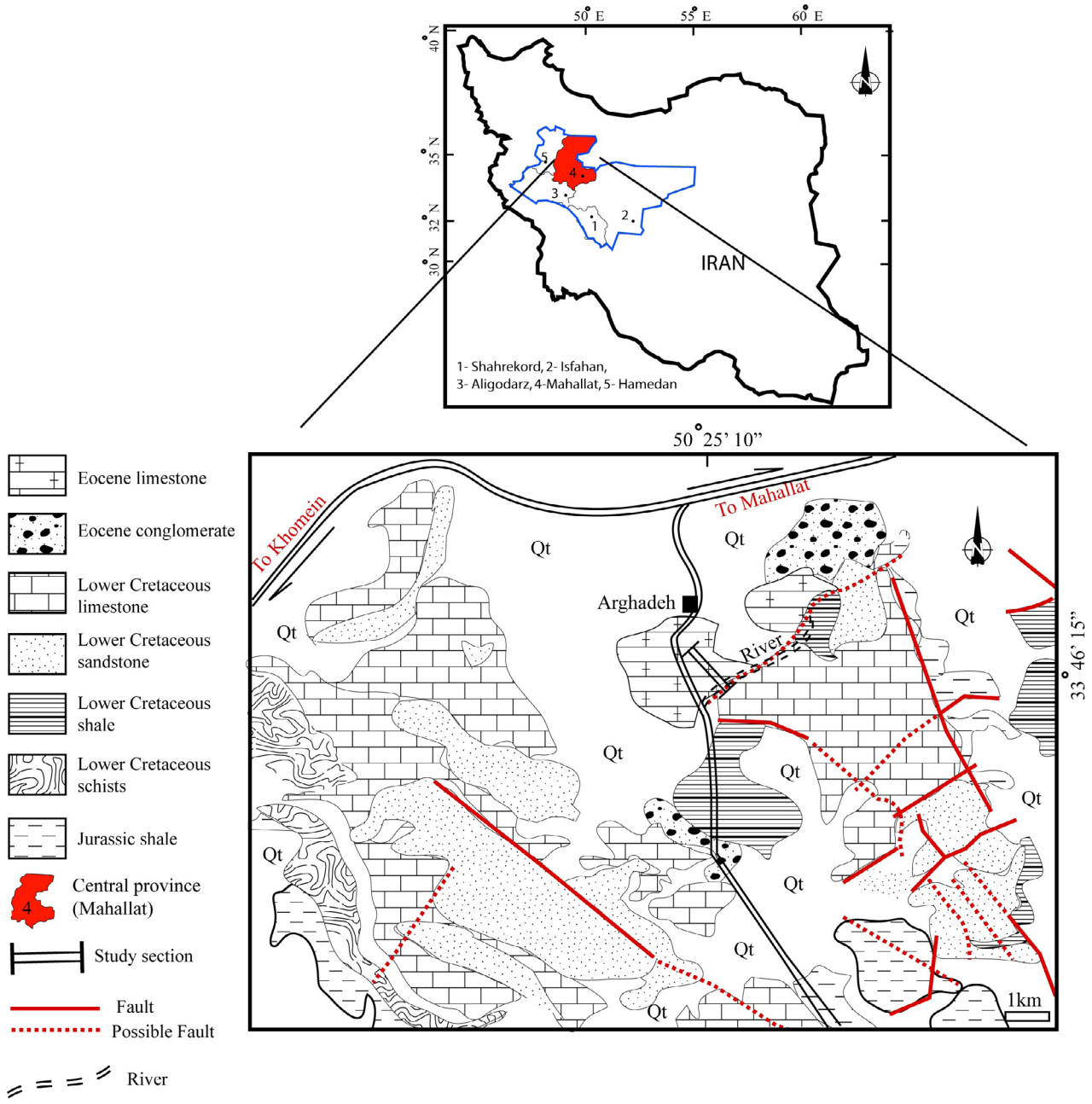

Figure 2. Location of the study area (Arghadeh area) on the Mahallat geological map, central Iran (Geological Survey of Iran) (Sheikholeslami, 2005).

In the study area, Eocene carbonate deposits consist of a succession of basal conglomerate, cream foraminiferal limestone including wackestone facies, massive coralgal limestone, and gray argillaceous limestone. The bioclasts are mainly composed of benthic foraminifers, bivalves (oysters), gastropod fragments, bryozoans, corals, and rare echinoids. The lower contact of this succession with Cretaceous deposits is discordant and the upper contact is covered by alluvium.

Among the 50 rock samples collected from the studied area, about 12 samples have new species. The numbers containing new species are as follows: 216, 217, 218, 220, 222, 223, 225, 230, 237, 238, 239, 240, and 241.

The measurements of axial and basal cone diameters (flattening index) were performed under the microscope with a micrometer and checked on photographic enlargements. For each parameter (cone diameter, spiral chambers, uniserial chambers, etc.) and flattening index (Rb/a) of the agglutinated conical taxa, a numerical statistic was provided and illustrated. The stratigraphic column and foraminiferal plate are done with Adobe Illustrator software. The suprageneric classification is established by Kaminski (2004, 2014) and the morphological terms of agglutinated foraminifers are used by the terminology of Hottinger & Drobne (1980).

All rock samples and thin sections in this study are stored in the paleontological collection (**Pc**) of the laboratory of Tehran Payame Noor University (**TPNU**).

Abbreviations: AZ I, rotaliids-valvulinids Assemblage Zone; **AZ II**, alveolinids-coskinolinids Assemblage Zone; **AZ III**, nummulitids-discocyclinids Assemblage Zone; **acd**, axial cone diameter, **bcd**, basal cone diameter, **Rb/a**, ratio between basal length and axial length (flattening index); **a**, aperture; **b**, beam; **ch**, chamber, **chm**, chamber margin; **cp**, continuous pillars;, **d**, depressed suture; **f**, foramen; **hb**, hemispherical base; **lsc**, last spiral chamber; **luc**, last uniserial chamber; **lw**, lateral wall; **ma**, marginal aperture; **mr**, marginal rim; **p**, pillar; **s**, septum; **ss**, spiral suture.

BIOSTRATIGRAPHY

The Early Eocene carbonate deposits containing rich benthic foraminifers are applied for establishing the biostratigraphical zonations. These deposits represent marine strata in the Mahallat region which were rarely studied and have poorly documented fauna.

No foraminiferal biozonation was established in the Mahallat region of the Neo-Tethyan High Zagros yet. Therefore, a systematic study of Eocene foraminiferal associations was carried out for the first time in the study area, which allowed the determination of three foraminiferal assemblages: rotaliids-valvulinids Assemblage Zone (**AZ I**), alveolinids-coskinolinids Assemblage Zone (**AZ II**), and nummulitids-discocyclinids Assemblage Zone (**AZ III**). They range from the middle Cuisian to early Lutetian (Figure 3).

FORAMINIFERAL ZONATIONS

Rotaliids-valvulinids Assemblage Zone (AZ I)

This assemblage occurs between the horizon (bed) 202 and the horizon (bed) 210 in stratigraphic order. This interval is 85 m thick and composed of a succession of carbonate facies that overlies the basal micro-conglomerate (Figure 3). It yields hyaline foraminifers such as *Granorotalia sublobata* Benedetti, Di Carlo & Pignatti, 2011, *Sphaerogypsina globulus* (Reuss, 1848), *Decrouezina aegyptiaca* (Cuvillier, 1930), *Assilina laxispira* De La Harpe, 1853, and *Nummulites* sp. together with rare small miliolids (*Biloculina* sp., *Triloculina* sp. and *Quinqueloculina* sp.). The biostratigraphic range is assigned to middle Cuisian based on the presence of marker species such as *Granorotalia sublobata* by Benedetti *et al*., 2011. This association is equivalent to the SBZ 11 (Serra-Kiel *et al*., 1998) and Tp 7b (BouDagher-Fadel *et al.*, 2015) (Figure 4).

Remarks. The biostratigraphic range of *Assilina laxispira* is attributed to Late Ypresian (Cuisian) by previous authors such as Samuel *et al*. (1972), Rahaghi & Schaub (1976), Serra-Kiel *et al*. (1998), and Saraswati *et al.* (2000, 2012). *Decrouezina aegyptiaca* is documented by Boukhary (1994) from the Upper Libyan Stage (Late Cuisian) at Beni Hassan (Nile Valley, Egypt). He again mentioned this species in his later work (Boukhary *et al*., 2009) from Early Eocene (Cuisian) Gebel Umm Russeies, Northern Galala, eastern desert (Egypt). *Granorotalia sublobata* was discovered and illustrated by Benedetti *et al.* (2011) in central and southern Italy. Its co-occurrence with other biostratigraphic markers such as *Alveolina decastroi* Scotto Di Carlo, 1966, *Alveolina cremae* Checchia-Rispoli, 1905 and *Cuvillierina vallensis* (Ruiz De Gaona, 1948), would confirm the middle Cuisian.

Alveolinids-coskinolinids Assemblage Zone (AZ II)

Further up, between beds 211 and 243, there is a carbonate succession of wackestone, about 275 m, containing two small patch reefs (Figure 3). The second foraminiferal assemblage (AZ II) occurs in this interval and is composed of abundant porcellaneous larger foraminifera (*Alveolina*) associated with agglutinated foraminifera (*Daviesiconus*, *Coleiconus*, *Coskinolina* Stache, *Barattolites*, *Cribrobulimina* Cushman, 1927, *Valvulina* d'Orbigny, 1826, *Pseudochrysalidina* Cole, 1941) and rare miliolids and rotalids (*Granorotalia*). This assemblage is subdivided into two sub-zones: A and B, based on the biostratigraphic range of the index *Alveolina*.

The sub-zone A is defined by the occurrence of *Alveolina distefanoi* Checchia-Rispoli, 1905, *A. decastroi*, *A. levantina* Hottinger, 1960 and *A. cremae.* Its biostratigraphic range is assigned to middle Cuisian and corresponds to the SBZ 11 (Serra-Kiel *et al*., 1998) and Tp 7b (BouDagher-Fadel *et al*., 2015) (Figure 4). The sub-zone B is characterized by the presence of *Alveolina frumentiformis* Schwager, 1883 and

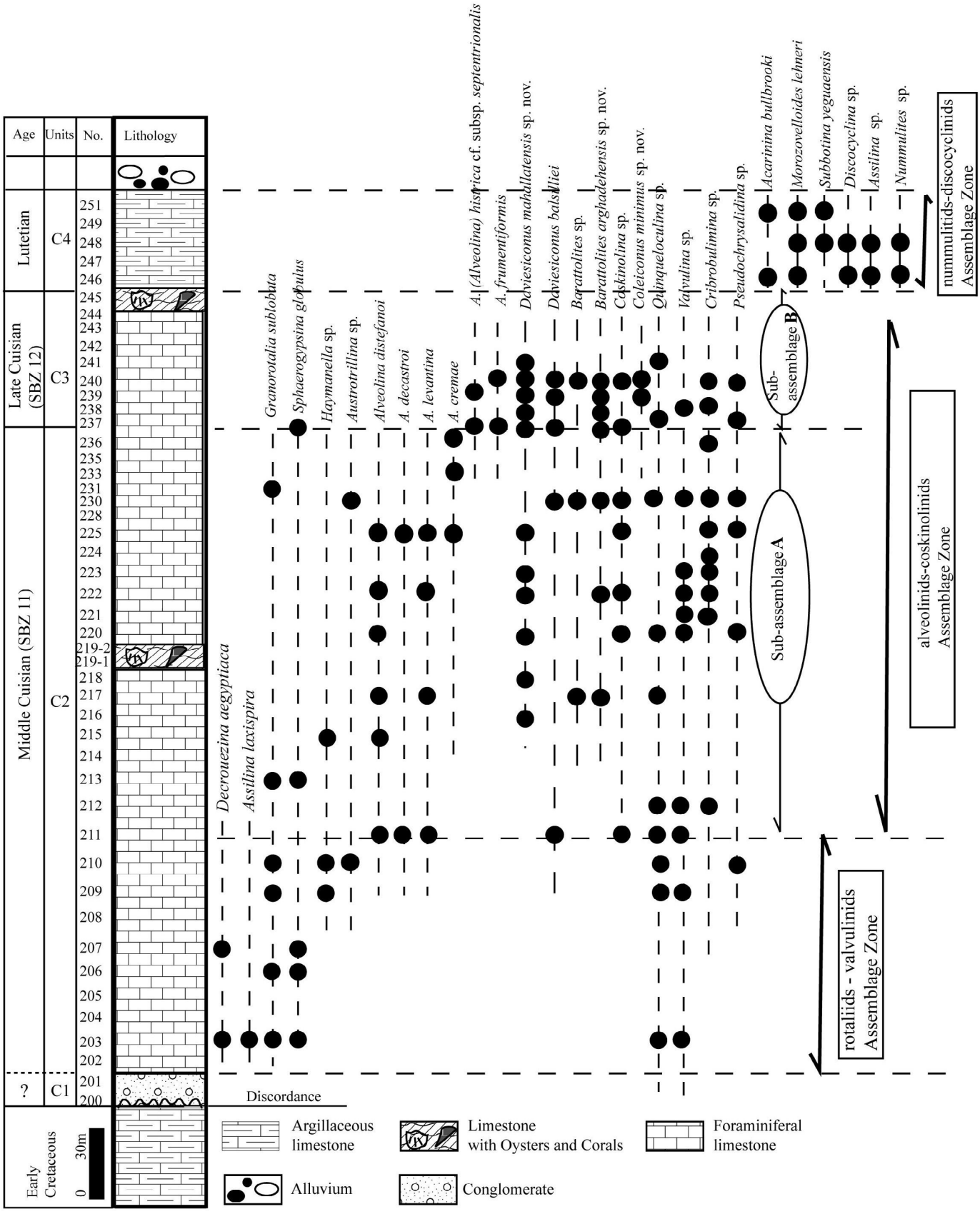

Figure 3. Distribution of selected foraminifera on the columnar stratigraphic section.

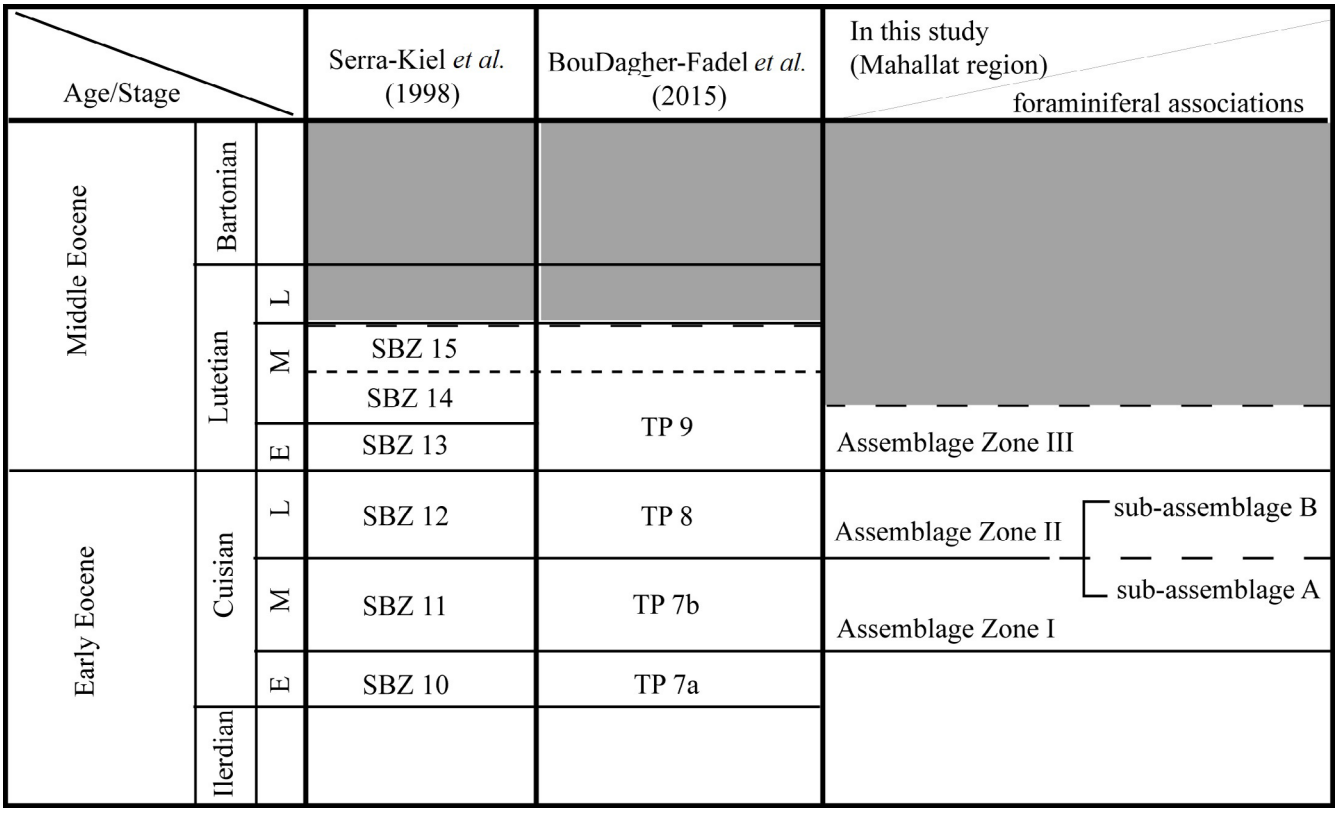

Figure 4. Correlation chart showing the biostratigraphic zonation of Serra-Kiel *et al*. (1998), BouDagher-Fadel *et al*. (2015), and foraminiferal assemblages in the studied area.

A. cf. *septentrionalis* Drobne, 1977. Its stratigraphic range is considered to late Cuisian age and corresponds to the SBZ 12 (Serra-Kiel *et al*., 1998) and Tp 8 (BouDagher-Fadel *et al*., 2015) (Figure 4). The three new species *Daviesiconus mahallatensis* sp. nov., *Coleiconus minimus* sp. nov., and *Barattolites arghadehensis* sp. nov. occur in this stratigraphic interval and are illustrated in Figure 3.

Nummulitids-discocyclinids Assemblage Zone (AZ III)

The third foraminiferal assemblage (AZ III) is recognized at the top of the studied section. This part of the section (between beds 246 to 251), about 40 m thick, consists of a succession of argillaceous limestone with large hyaline foraminifera (*Discocyclina* sp., *Assilina* sp.) and planktonic foraminifera such as *Acarinina bullbrooki* (Bolli, 1957), *Morozovelloides lehneri* (Cushman & Jarvis, 1929), and *Dentoglobigerina yeguaensis* (Weinzierl & Applin, 1929). This assemblage zone is assigned to the Middle Eocene (early Lutetian) based on the planktonic foraminifers (Berggren *et al*., 2006; Hayward *et al*., 2022).

SYSTEMATIC PALEONTOLOGY

Class FORAMINIFERA D'Orbigny, 1826
Subclass TEXTULARIIA Mikhalevich, 1980
Order LOFTUSIIDA Kaminski & Mikhalevich, 2004, in Kaminski, 2004)
Suborder LOFTUSIINA Kaminski & Mikhalevich, 2004
Superfamily LOFTUSIACEA Brady, 1884
Family ORBITOLINIDAE Martin, 1980

Daviesiconus Hottinger & Drobne, 1980

Daviesiconus mahallatensis sp. nov.
urn:lsid:zoobank.org:pub:98AC9DA3-360B-471A-BD70-892FCFD73931
(Figures 5, 6A–B; 7A–I)

Diagnosis. The test is characterized by the finely agglutinated conical shell with low trochospiral chambers arrangement in the early growth stage. The exoskeleton is composed of

Species	*Daviesiconus mahallatensis* sp. nov. bcd > acd					*Daviesiconus balsilliei* (Davies, 1930) bcd ≃ acd					*Barattolites arghadehensis* sp. nov. bcd < acd				
Samples	acd (mm)	bcd (mm)	R b/a av.= 1.22	spiral chambers	uniserial chambers	acd (mm)	bcd (mm)	R b/a av.= 1	spiral chambers	uniserial chambers	acd (mm)	bcd (mm)	R b/a av.= 0.42	spiral chambers	uniserial chambers
216-1	1.65	2.125	1.28	3-4	9-10										
218-1	1.3	1.56	1.2	——	7-8										
220-1 (megalosph.)	0.35	0.45	1.28	2-3	——										
222-1 (megalosph.)	0.56	0.63	1.12	2-3	3										
223-1	1. 37	1.62	1.2	——	——										
225-1	1.05	1.125	1.1	——	——										
238-1	1.1	1.55	1.4	——	——										
241-1	1.25	1.4	1.12	4-5	8										
241-2	1.06	1.5	1.4	——	——	*Daviesiconus balsilliei*									
230-1	—	—	—	—	—	1.3	1.27	0.97	3-4	8-9					
237-1	—	—	—	—	—	1.56	1.55	0.99	3-4	8-9					
239-2	—	—	—	—	—	1.44	1.40	0.97	3-4	7-8					
240-1	—	—	—	—	—	1.06	1	0.94	3-4	8-9	*Barattolites arghadehensis* sp. nov.				
222-2	—	—	—	—	—	—	—	—	—	—	1.4	0.56	0.40	5-6	7-8
238-2	—	—	—	—	—	—	—	—	—	—	1.3	0.56	0.43	4-5	6-7
239-3	—	—	—	—	—	—	—	—	—	—	1.44	0.65	0.45	5-6	7-8
240-5	—	—	—	—	—	—	—	—	—	—	1.52	0.60	0.40	5-6	7-8

Samples	acd (mm)	bcd (mm)	R b/a av.= 1.14	spiral chambers	uniserial chambers
	Coleiconus minimus n. sp.				
239-1	0.875	1	1.15	3-4	5-6
239-4	0.85	0.95	1.1	——	——
239-5	1.06	1.125	1		
240-3	0.87	1.06	1.2	3-4	6-7
240-4	1.125	1. 25	1.1	3-4	5-6
240-6	0.65	0.80	1.2	——	——
240-7	0.75	0.875	1.16	——	——
240-8	1.125	1. 25	1.1	3-4	6-7

A

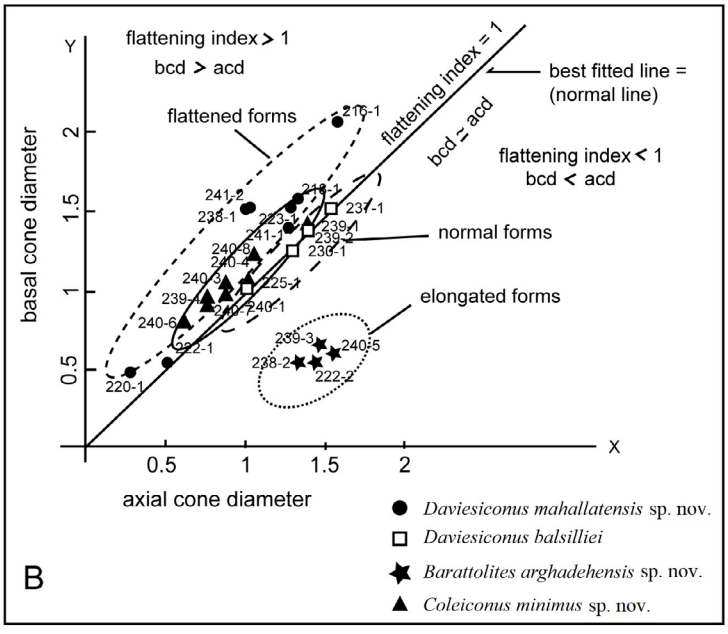

B

Figure 5. A, biometrical comparison between four agglutinated conical foraminifera: *Daviesiconus mahallatensis* sp. nov., *Barrattolites arghadehensis* sp. nov., *Coleiconus minimus* sp. nov., and *Daviesiconus balsilliei*; **B**, flattening index diagram for aforementioned agglutinated conical foraminifera.

simple radial partitions (beams) without intercalary beams and rafters. The endoskeleton is composed of continuous pillars from one chamber to the next one. The cone base is slightly convex in the adult stage and larger than its height. The basal margin shows marginal rims in the adult stage.

Derivation of name. The specific name refers to Mahallat City, central Iran.

Holotype. Illustrated in Figures 6A–B.

Type locality. East Arghadeh village, Mahallat City, Central Iran.

Stratigraphic level. Early Eocene (Cuisian) (SBZ 11–12).

Repository. Deposited at the TPNU (Tehran Payame Noor University), Tehran, Iran. The number of samples is 216, 218, 220, 222, 223, 225, 237, 238, 239, 240, and 241.

Description. Finely agglutinated shell with low trochospiral chambers arrangement in the early growth stage and followed by uniserial chambers arrangement with distinctly depressed sutures in the adult stage. The axial and basal cone diameters (axial and basal lengths) reach 1.65 mm and 2.125 mm respectively, for the holotype (Figures 6A–B). The ratio between the basal length and axial length (flattening index, Rb/a) is 1.28 for the holotype. In the collected material, the axial cone diameter (acd) ranges between 1 and 1.37 mm, and the basal cone diameter (bcd) is between 1.125 and 1.62 mm. The average flattening index is 1.2. This new species is located on the left side of the normal line of the flattening index diagram (Figure 5B). The conical test is wider than its height and the basal margin shows a specific marginal rim in the adult stage. There are three to four chambers in a low-trochospiral arrangement of the nepionic stage for the holotype. There are 6–7 uniserial chambers per 1 mm of axial length. The cone base is slightly convex with a hemispherical view in both the nepionic and adult stages. The microspheric forms are poorly known because the embryonic apparatus is not clear. The megalospheric form is found in a more eccentric position followed by a loosely coiled nepionic stage. The diameter of axial and basal cones is 0.35 and 0.45 mm respectively. The ratio between the basal and axial cone diameters (Rb/a) varies from 1–1.4 in the megalospheric specimens. The megalospheric proloculus is eccentric and followed by hemispherical deuteroconch and a few (2–3) coiled chambers. The exoskeleton consists of simple radial partitions (beams) without intercalary beams and rafters. The endoskeleton consists of continuous pillars from one chamber to the next one. The pillars are subcircular in horizontal sections. The apertural face is arranged by a few relatively large pores with marginal apertures and marginal rims at the periphery. The morphometric data and the dimensional comparison of the new taxon are figured out and plotted in Figures 5A–B.

Remarks. *Daviesiconus* is close to the genus *Barattolites* due to the trochospiral nepionic stage in both generations and simple exoskeleton; however, it differs in the presence of marginal apertures, small trochospiral early growth stage, and absence of intercalary beams. This new species differs from *Daviesiconus balsilliei* in the low-trochospiral stage with a slightly eccentric position, wide cone base, bell-shaped test with marginal rims, and greater flattening index. It is associated with *Alveolina distefanoi*, *A. decastroi*, *A. levantina*, *A. cremae*, *A. frumentiformis*, and *A.* cf. *septentrionalis*. Therefore, its biostratigraphic range extends from the Middle Cuisian to the Late Cuisian.

Daviesiconus Hottinger & Drobne, 1980

Daviesiconus balsilliei (Davies, 1930)
(Figures 7J–O)

1930 *Coskinolina balsilliei* Davies, p. 496; pl. 1, figs. 6–9; pl. 2, figs. 4–6 and 15.
1939 *Coskinolina liburnica* Stache, Silvestri, pl. 6, figs. 5? 6–7; pl. 8, figs. 4–5; pl. 20, fig. 5.
1948 *Coskinolina balsilliei* Davies, Henson, p. 29; pl. 7, fig. 10; pl. 10, fig. 11.
1970 *Coskinolina balsilliei* Davies, Kaever, p. 24; pl. 2, figs. 6, 8–9.
1980 *Fallotella* (*Daviesiconus*) *balsilliei* (Davies), Hottinger & Drobne, p. 242–243; text-fig. 4; pl. 17, figs.1–23.
2015 *Daviesiconus balsilliei* (Davies), Garcia, p. 105; text-fig. 4.25(1–14).
2016 *Daviesiconus balsilliei* (Davies), Serra-Kiel1 *et al*., p. 50; text-fig. 35(1–14).

Description. The agglutinated conical test shows a small embryonic apparatus with trochospiral early growth stage followed by the arrangement of uniserial chambers with slightly depressed sutures in the adult stage. The embryonic apparatus is eccentric and composed of a protoconch and a prominent hemispherical deuteroconch. The cone base is slightly convex with a hemispherical view in both nepionic and adult stages. The thick wall has a pseudokeriothecal texture. The axial cone diameter (acd) ranges between 1.06 mm and 1.56 mm and the basal cone diameter (bcd) between 1 mm and 1.55 mm. This specimen is almost isometric with a ratio between basal length and axial length (flattening index, Rb/a) of approximately 1 in megalospheric form. This species plots on the normal line of the flattening index diagram (Figure 5B). In the collected materials, there are 6–7 uniserial chambers per 1 mm axial cone diameter in adult form. The endoskeleton consists of pillars continuous from one chamber to the next one. The exoskeleton displays simple radial partitions (beams) without intercalary beams and rafters. This structure along with some parts of the endoskeleton is described as septula by Hottinger (2007). The outline of the pillars is subcircular to circular in the horizontal section. The apertural face is arranged by a few relatively large pores with marginal apertures in the periphery (Hottinger & Drobne, 1980).

Remarks. According to Hottinger & Drobne (1980), the diameter of axial and basal cones of *Daviesiconus balsilliei* measures 0.75–1.325 mm and 1–1.75 mm respectively, in megalospheric form. For a basal cone diameter of 1.5 mm,

there are 6–8 radial partitions per quadrant. There are 8 pillars per 1.5 mm on an axial cone-diameter. There are 7–8 uniserial chambers per 1 mm on a cone axial line for this specimen. The stratigraphic range of the material's Hottinger & Drobne is assigned to the Early Eocene in the Middle East.

According to Serra-Kiel *et al*. (2016) The megalospheric form of *Daviesiconus balsilliei* has axial and basal cone diameters of 2.75 mm and 2.3 mm respectively, in Dhofar (Oman) and Socotra Island (Yemen) sections. Whereas in microspherical form, the conical test has a maximum axial diameter of 4.9 mm and a maximum basal diameter of 4.8 mm. Based on the foregoing data, the test of *D. balsilliei* seems to be isometric. This species is associated with *Nummulites cyrenaicus* Schaub, 1981, *N. vicaryi* d'Archiac & Haime, 1853, and *N. fabianii* Prever, 1905 assigned to the upper Bartonian to Priabonian SBZ18-20 in Yemen.

Therefore, it seems that the recorded species is close to the specimens of *Daviesiconus balsilliei* collected from former Yugoslavia (Hottinger & Drobne, 1980), but it differs from those of Oman and Yemen (Serra-Kiel *et al.*, 2016) in the smaller test size of the test and fewer uniserial chambers per 1mm axial cone-diameter. Based on biometric measurements, the figured specimens of *D. balsilliei* of Hottinger & Drobne (1980) are smaller than those found in the materials of Serra-Kiel *et al*. (2016). This species is associated with *Alveolina distefanoi*, *A. decastroi*, *A. levantina*, *A. frumentiformis*, and *A.* cf. *septentrionalis*. Thus, its biostratigraphic range extends from the middle Cuisian to the late Cuisian.

Barattolites Vecchio & Hottinger, 2007

Barattolites arghadehensis sp. nov.
urn:lsid:zoobank.org:pub:502D0601-96E3-407C-A6C2-98A642D841E4
(Figures 6C–D; 8A–I)

Diagnosis. The conical agglutinated test has a planispiral chamber arrangement in the early stage and continue with low trochospiral. It consists of three parts, apical with the embryonic chambers, middle with spiral chambers, and lower with uniserial chambers. The cone base is almost flat and slightly convex in the adult stage. The exoskeleton consists of beams and intercalary beams arranged in a line or alternated from one chamber to the next. The endoskeleton is composed of continuous pillars with an irregular pattern while marginal apertures are not observed.

Derivation of name. The specific name refers to Arghadeh village, Mahallat City, central Iran.

Holotype. Illustrated in Figures 6C–D.

Type locality. East Arghadeh village, Mahallat City, Central Iran.

Stratigraphic level. Early Eocene (Cuisian) (SBZ 11–12).

Repository. Deposited at the TPNU (Tehran Payame Noor University). Tehran, Iran. The number of samples is 217, 222, 230, 237, 238, 239, and 240.

Description. The conical agglutinated test has an embryonic apparatus in an eccentric position. The proloculus with a planispiral chamber arrangement and low trochospiral in the early stage is followed by 5–6 spiral chambers in the nepionic stage and continued by 7–8 uniserial chambers with slightly depressed sutures in the later stage. There are 5–6 uniserial chambers per 1 mm of axial length. The nepionic stage shows an inclined position with respect to the axes of the adult cone. In the microspheric form, the new species has an axial cone diameter of 1.44 mm and the basal cone diameter of 0.65 mm for the holotype (Figures 6C–D). The flattening index (Rb/a) is 0.45. The remaining specimens have an axial cone diameter of 1–1.4 mm, and a basal cone diameter of 0.5–0.6 mm. The average flattening index (Rb/a) is 0.42. This new species is located on the right side of the normal line of the flattening index diagram (Figure 5B). The conical shell is subdivided into three parts based on its morphological appearance: the apical part with a narrow apical angle in the early stage, the middle part with spiral chambers in the nepionic stage, and the lower part with uniserial chambers in the neanic stage. The cone base is almost flat and slightly convex in the adult stage. The chamber sutures are slightly depressed. The microspheric form shows an eccentric position with tight trochospiral chambers in the early stage and followed by trochospiral chambers arrangement in the spiral stage and uniserial chambers in the adult stage. The megalospheric form has an embryonic apparatus that may be considerably inclined with respect to the axis of the adult cone. The nepionic growth stage is composed of 4–5 chambers in a short trochospiral arrangement and the neanic growth stage is composed of 2–3 uniserial chambers. The endoskeleton consists of continuous pillars which represent an irregular pattern and are positioned in the adaxial zone. Marginal apertures are not observed. The exoskeleton consists of beams and intercalary beams arranged in a line or alternated from one chamber to the next (Figures 8D–E). The morphometric data and the dimensional comparison of the new taxon are figured and plotted in Figures 5A–B.

Remarks. The genus *Barattolites* is distinguished by the simple exoskeleton with beams and intercalary beams and the absence of marginal apertures and rafters. The *Barattolites arghadehensis* sp. nov. differs from the *B. trentinarensis* and *B. andhuri* Gallardo-Garcia & Serra-Kiel, 2016 in a smaller size of the test, narrower apical angle, and presence of small planispiral juvenile growth stage with low-trochospiral chamber arrangement in the early stage.

The *Barattolites trentinarensis* is reported so far from Trentinara Formation (southern Italy) and Jahrum Formation (southern Iran) (Hottinger, 2007; Vecchio & Hottinger, 2007). In the materials of southern Italy, the agglutinated conical test of *B. trentinarensis* reaches about 3 mm of axial cone diameter in microspheric forms and about 2 mm in megalospheric forms. The flattening index is 0.5 in megalospheric form and 0.7 in microspheric specimens. In the Iranian specimens collected by Rahaghi (1980) from the south and east Iran, there are 7–8 uniserial chambers per 1 mm on a cone axial line. According to Hottinger (2007), the Italian specimens are slenderer in shape than the Iranian specimens (Rahaghi's materials).

Figure 6. Drawing of thin sections of three new species. **A–B**, *Daviesiconus mahallatensis* sp. nov., **A**, axial section, thin section: 216; **B**, Camera Lucida drawing with indication of structural elements, Early Eocene (Cuisian), Arghadeh area (Mahallat region). **C–D**, *Barrattolites arghadehensis* sp. nov., **C**, axial section, thin section: 239; **D**, Camera Lucida drawing with indication of structural elements, Early Eocene (Cuisian), Arghadeh area (Mahallat region). **E–F**, *Coleiconus minimus* sp. nov., **E**, axial section, thin section: 240; **F**, Camera Lucida drawing with indication of structural elements, Early Eocene (Cuisian), Arghadeh area (Mahallat region). **Abbreviations: a**, aperture; **b**, beam; **ch**, chamber; **cp**, continuous pillars; **ds**, depressed suture; **hb**, hemispherical base; **lsc**, last spiral chamber; **luc**, last uniserial chamber; **lw**, lateral wall; **ma**, marginal aperture; **mr**, marginal rim; **p**, pillar; **s**, septum. Scale bars: A = 1 mm; C, E = 0.5 mm; B, D, F = without scale bar.

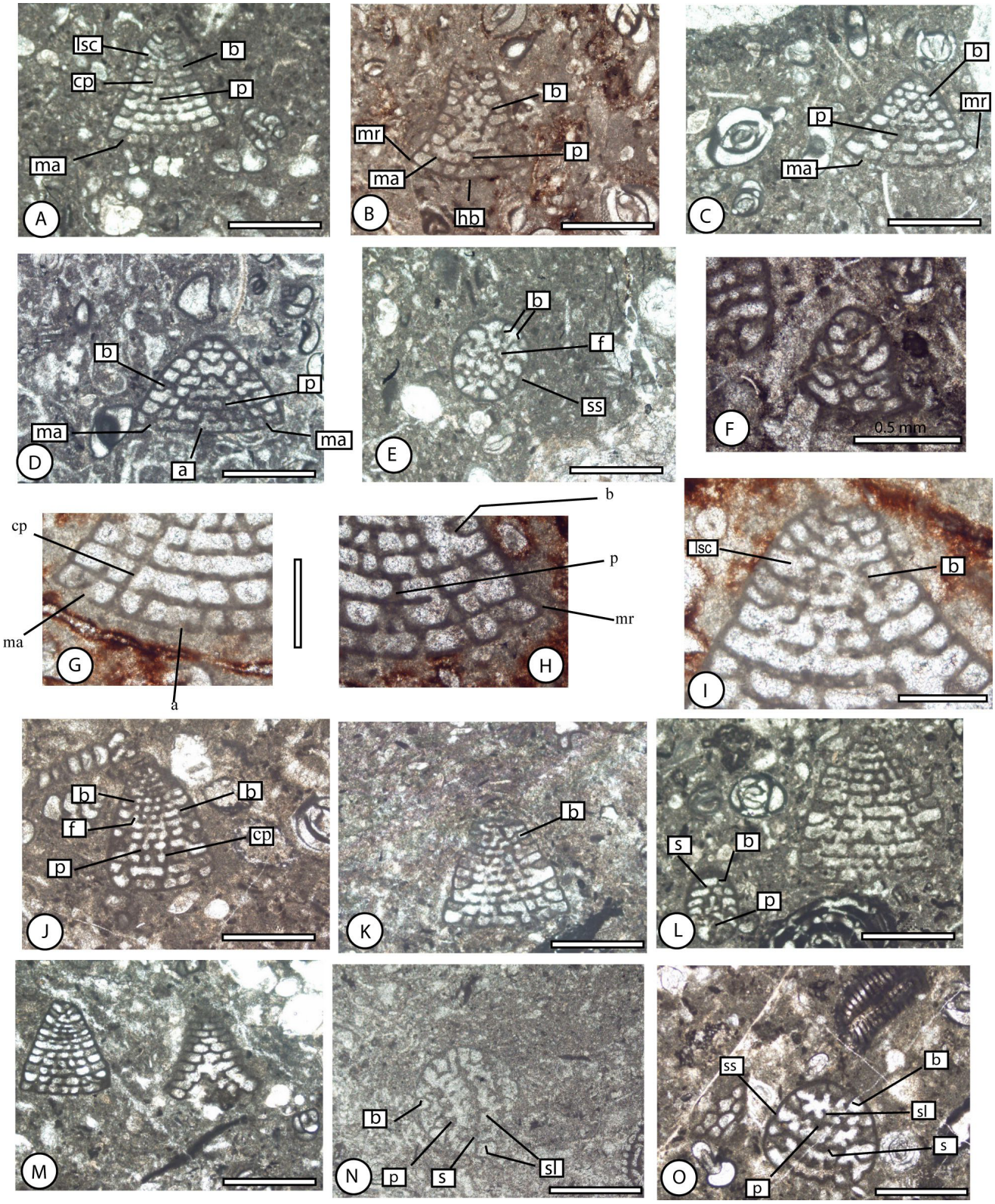

Figure 7. Photographs of foraminiferal species. **A–I**, *Daviesiconus mahallatensis* sp. nov., **A**, thin section 241–1, axial section; **B**, thin section 218–1, subaxial section; **C**, thin section 241–2, oblique section; **D**, thin section 238–1, oblique section; **E**, thin section 241–4, basal section; **F**, thin section 222–1, axial section, megalospheric form; **G**, **H**, thin section 216–1, detail showing a wall texture; **I**, thin section 216, axial section. **J–O**, *Daviesiconus balsilliei*, J, thin section 230–1, subaxial section; **K**, thin section 239–2, subaxial section; **L**, thin section 237–1, upper right: subaxial section and lower left, *Daviesiconus mahallatensis* sp. nov., basal oblique section; **M**, left, thin section 240–1, subaxial section and right, *Barattolites* sp., subaxial section; **N**, thin section 211–1, basal oblique section; **O**, thin section 230–2, basal oblique section. All specimens are collected from Arghadeh area (Mahallat region). **Abbreviations: a**, aperture; **b**, beam; **ch**, chamber; **cp**, continuous pillars; **ds**, depressed suture; **f**, foramen; **hb**, hemispherical base; **lsc**, last spiral chamber; **luc**, last uniserial chamber; **lw**, lateral wall; **ma**, marginal aperture; **mr**, marginal rim; **p**, pillar; **s**, septum. Scale bars: A–E, L–M = 1 mm; F–I = 0.5 mm.

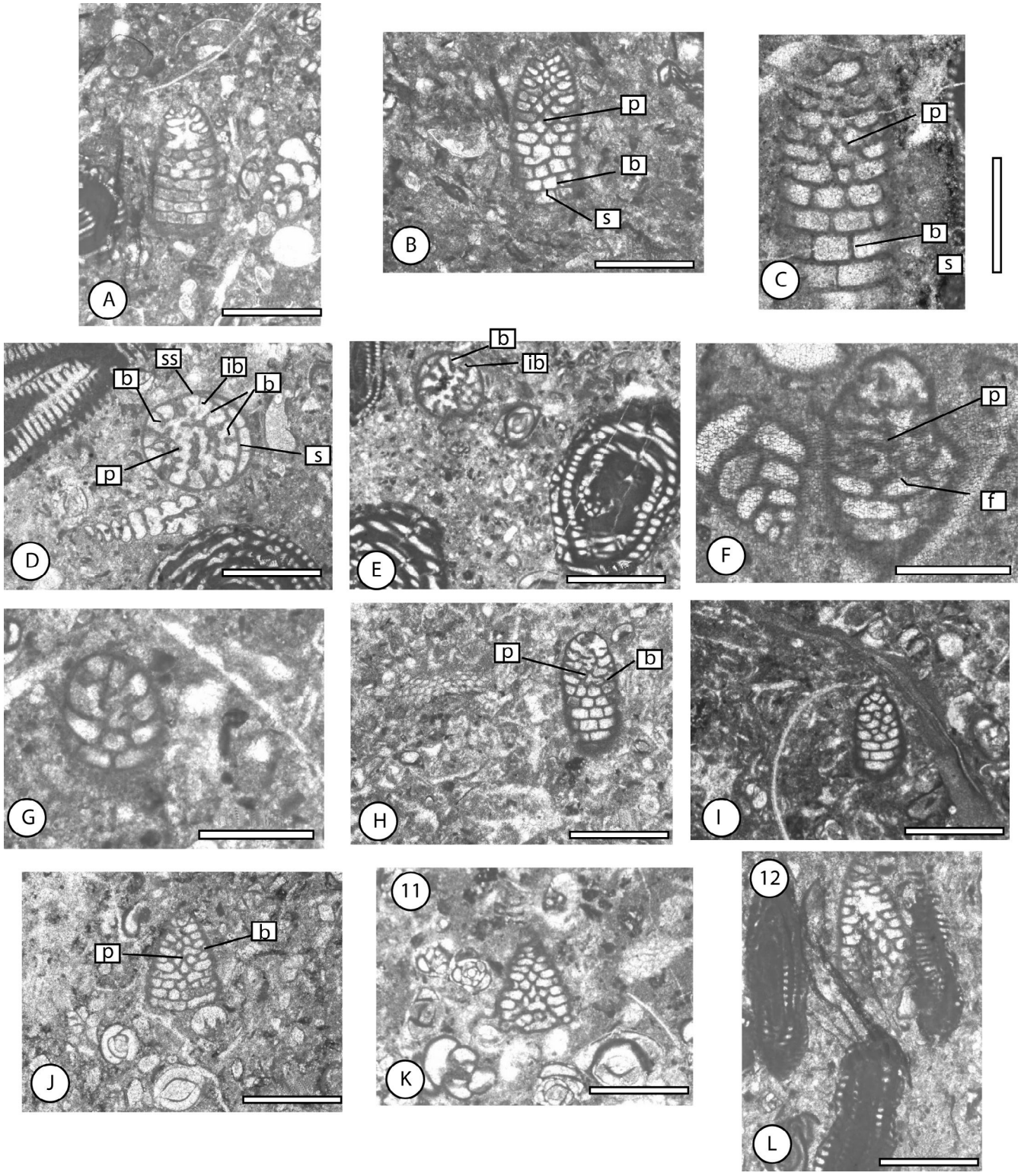

Figure 8. Photographs of foraminiferal species. **A–I**, *Barrattolites arghadehensis* sp. nov., **A**, thin section 239–3, axial section; **B**, thin section 240–5, subaxial section; **C**, thin section 222–2, subaxial section; **D**, thin section 237–3, basal oblique section; **E**, thin section 237–4, basal oblique section; **F**, thin section 230–3, subaxial section, megalospheric form; **G**, thin section 239–4, axial section, megalospheric form; **H**, thin section 238–2, subaxial section; **I**, thin section 238–3, subaxial section. **J–L**, *Barrattolites* sp., **J**, thin section 217–1, subaxial section; **K**, thin section 230–4, subaxial section; **L**, thin section 240–8, subaxial section. All specimens are collected from Arghadeh area (Mahallat region). Scale bars: A–B, D–E, G–L = 1 mm; C, F = 0.5 mm. Abbreviations: **b**, beam; **f**, foramen; **p**, pillar; **s**, septum.

It is believed that the *Barattolites arghadehensis* sp. nov. is an ancestral form of *B. trentinarensis* because it is smaller and has an early planispiral stage in the early apical system. This new species is associated with *Alveolina distefanoi*, *A. decastroi*, *A. levantina*, *A. frumentiformis*, and *A.* cf. *septentrionalis* indicating middle to late Cuisian.

Barattolites Vecchio & Hottinger, 2007

Barattolites sp.
(Figures 8J–L)

Description. The agglutinated test shows a high-conical morphology with a slightly convex base. The wall is thick with a pseudokeriothecal texture. No microspheric forms were found. The axial cone-diameter ranges between 1 and 1.4 mm and the basal cone diameter between 0.65 and 0.75 mm. The average flattening index of this species is 0.67. This species is located on the right side of the normal line.

Remarks. The *Barattolites* sp. is similar to *Barattolites andhuri*, due to the equilateral triangular outline but differs in its smaller test size of the test. This species differs from *Barattolites arghadehensis* sp. nov. in the larger average flattening index, larger basal cone diameter, and the equilateral triangular outline in the axial section. The *Barattolites* sp. differs from the *B. trentinarensis* in a smaller test size of the test and the presence of an equilateral triangular outline. According to Vecchio & Hottinger (2007), the stratigraphic range of *B. trentinarensis* covers the Ypresian to the Early Lutetian (Vecchio & Hottinger, 2007), whereas this recorded species, like *Barattolites arghadehensis* sp. nov., was found in the middle to late Cuisian deposits. It is associated with *Alveolina frumentiformis*, *A. distefanoi*, *A. levantina*, *Daviesiconus balsilliei* and *Cribrobulimina* sp.

Coleiconus Hottinger & Drobne, 1980

Coleiconus minimus sp. nov.
urn:lsid:zoobank.org:pub:D0A7421E-CEB6-442F-87BD-16F492C637E0
(Figures 9A–I)

Diagnosis. The agglutinated conical test presents an eccentric prominent trochospiral chamber in the early stage. The thick wall shows pseudokeriothecal texture with distinctly depressed sutures. The cone base is convex in the adult stage. The exoskeleton is characterized by a simple structure with thick beams and without intercalary beams and rafters. The endoskeleton is composed of discontinuous pillars arranged in a wide space.

Derivation of name. This species has a small test.

Holotype. Illustrated in Figures 6E–F.

Type locality. East Arghadeh village, Mahallat City, Central Iran.

Stratigraphic level. Early Eocene (Cuisian) (SBZ 11-12).

Repository. Deposited at the TPNU (Tehran Payame Noor University), Tehran, Iran. The number of samples is 239 and 240.

Description. The agglutinated conical test has a prominent early trochospiral stage in an eccentric position and is followed by the uniserial arrangement of chambers with distinctly depressed sutures in the adult stage. The conical test is characterized by a thick wall with pseudokeriothecal texture, distinctly depressed sutures, and a convex cone base in the adult stage. The diameter of axial and basal cones are 0.87 mm and 1.06 mm respectively, for the holotype (Figures 6E–F). The flattening index (Rb/a) is 1.22 for the holotype. In the other material, the axial cone diameter (acd) ranges between 0.65 and 1.125 mm, and the basal cone diameter (bcd) is between 0.8 and 1.25 mm. The average flattening index is 1.14. This new species is located on the left side and near the normal line (Figure 5B). No microspherical forms were found. The endoskeleton consists of discontinuous pillars arranged in a wide space. The exoskeleton presents a simple structure with thick beams and without intercalary beams and rafters. The apertural face is arranged by large pores with marginal apertures. This new species is associated with *Alveolina frumentiformis*, and *A.* cf. *septentrionalis*. Its biostratigraphic range is late Cuisian. The morphometric data and the dimensional comparison of the new taxon are figured out and plotted in Figures 5A–B.

Remarks. The genus *Coleiconus* is distinguished from *Barattolites* by possessing a thick marginal wall with a keriothecal structure, distinct marginal trough with a row of marginal apertures, a much more prominent spiral stage, and coarse internal structure with the large chamberlets in the marginal zone. *Coleiconus minimus* sp. nov. differs from *Coleiconus elongata* (Cole, 1942) and *Coleiconus zansi* Robinson, 1993 in a smaller size, convex cone base, and more prominent spiral stage. This species is close to *Coleiconus christianaensis* Robinson, 1993, but differs in a finner internal structure and looser aspect of the central pillars. This new species is associated with *Alveolina frumentiformis*, and *A.* cf. *septentrionalis*. Its biostratigraphic range is late Cuisian.

In the materials of Hottinger & Drobne (1980), *Coleiconus elongata* has maximum axial and basal diameters of 1.6 mm and 2 mm, respectively. There are 6 pillars per 1.5 mm on a cone diameter and 8–9 uniserial chambers per 1 mm on a cone axial line for this species. The flattening index is 0.6–1.2. In Rahaghi's materials (Rahaghi, 1980), from the south and east Iran, there are some specimens similar to *Daviesiconus* and *Coleiconus*. In comparison with the samples collected from the studied area, Rahaghi's specimens have simple radial partitions (beams), but were identified as *Coskinolina* sp. nov. from the Sabzewar area (Rahaghi, 1980). They are associated with *Alveolina stercusmuris* Mayer-Eymar, 1886, *A. frumentiformis*, and *Nummulites laevigatus* (Bruguière, 1792), which are assigned to the Middle Eocene in the Sabzewar area. Its age is deduced from the faunal associations.

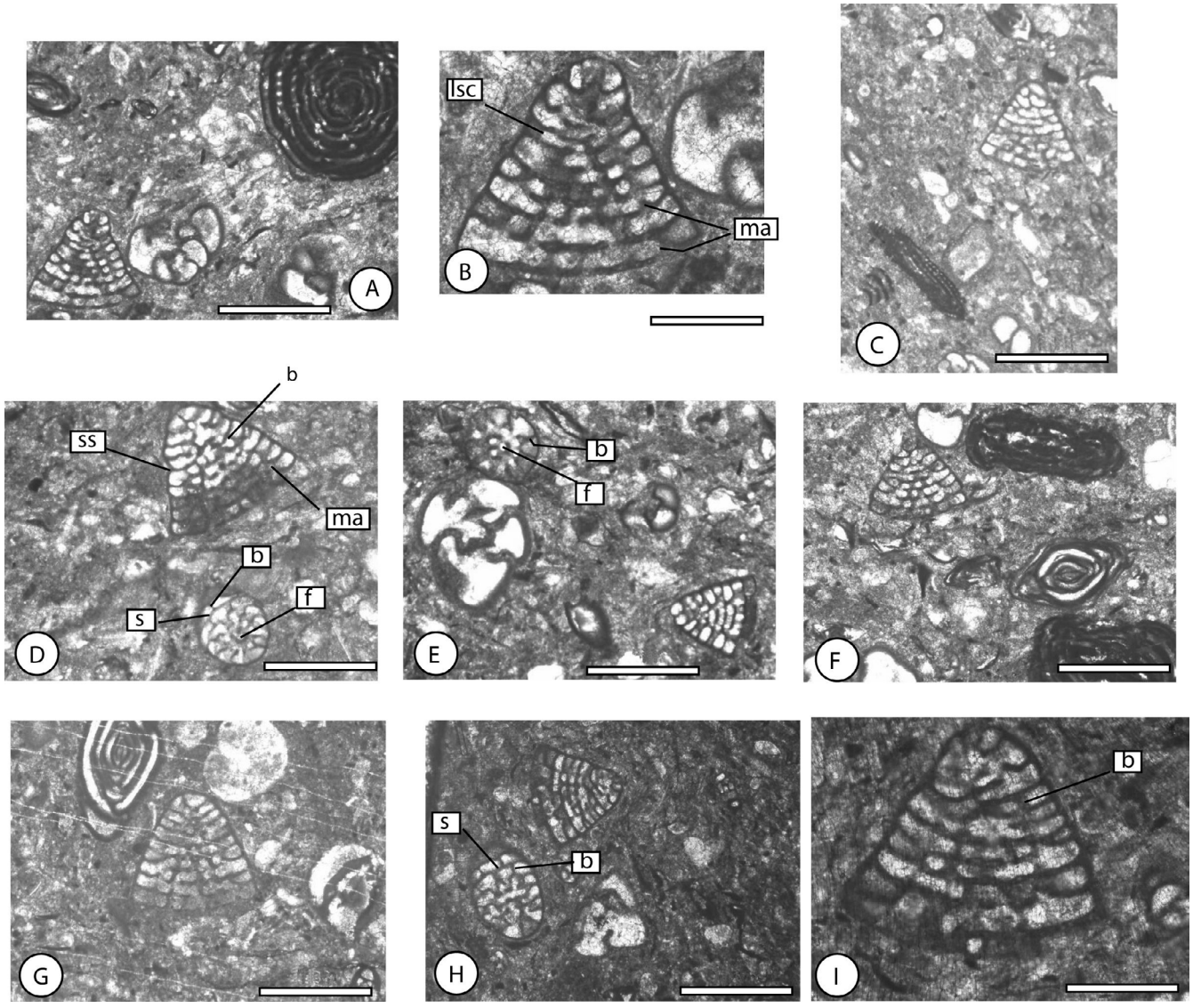

Figure 9. Photographs of foraminiferal species. **A–I**, *Coleiconus minimus* sp. nov., **A–B**, thin section 240–3, axial section; **C**, thin section 239–4, subaxial section; **D**, thin section 240–4, upper: subaxial section and lower: basal oblique section; **E**, thin section 240–6, upper left: basal oblique section and lower right: subaxial section; **F**, thin section 240–7, subaxial section; **G**, thin section 239–5, subaxial section; **H**, thin section 239–1, upper: subaxial section and lower: basal oblique section; **I**, thin section 239–1, subaxial section. All specimens are collected from Arghadeh area (Mahallat region). **Abbreviations: b**, beam; **f**, foramen; **lsc**, last spiral chamber; **ma**, marginal aperture; **p**, pillar; **s**, septum; **ss**, spiral suture. Scale bars: A, C–H = 1mm; B, I = 0.5 mm.

DISCUSSION

Integrated micropaleontological and stratigraphical studies on Paleogene carbonate rocks provide new knowledge on the foraminiferal associations and stratigraphic range in the studied area. From the point of view of biostratigraphy, three foraminiferal assemblages are presented in the Mahallat region for the first time. They consist of rotaliids-valvulinids Assemblage Zone (AZ I), alveolinids-coskinolinids Assemblage Zone (AZ II), and nummulitids-discocyclinids Assemblage Zone (AZ III). Based on the biostratigraphic foraminiferal marker, the first assemblage (rotaliids-valvulinids Assemblage Zone) is equivalent to the SBZ 11 (Serra-Kiel *et al*., 1998). This assemblage occurs in the lower part of the studied section and is assigned to the middle Cuisian. The second assemblage (alveolinids-coskinolinids Assemblage Zone) is characterized by the presence of abundant alveolinids which allowed me to determine two sub-zones: A and B in the middle part of the studied section. The biostratigraphic range of each sub-zone corresponds to the SBZ 11 and 12 and is assigned to middle and late Cuisian respectively. The planktonic foraminifers presented in the third assemblage (nummulitids-discocyclinids Assemblage Zone) are considered marker fossils, but the benthic foraminifers have never been an indicator for the biostratigraphic scheme. In this work, due to the stratigraphic location and the concurrent range of the recorded planktonic

foraminifers, the biostratigraphic range of this assemblage is attributed to the Lutetian stage.

From the point of view of paleoecology, the rotaliids-valvulinids Assemblage Zone (AZ I), is dominated by the local enrichment of small miliolids and small rotaliids with few large, flat, thin layer hyaline foraminifers (*Assilina* and *Decrouezina*). The presence of miliolids in the fine grain wackestone indicates an oligotypic community and corresponds to locally restricted conditions with enhanced nutrients in shallow water (Geel, 2000). The small rotaliids are considered to be very frequent in calcareous littoral deposits from the inner neritic zone (lagoon) to shallow protected subtidal setting (Luterbacher, 1984; Accordi *et al*., 1998; Ozgen-Erdem *et al*., 2005). Whereas the thin layer *Assilina* d'Orbigny, 1839 is adapted to stable, slightly nutrient-depleted environments, normal marine salinity values, the lower limit of the photic zone, and deeper environment (*i.e*., deeper part of the photic zone) (Racey, 1994).

In alveolinids-coskinolinids Assemblage Zone (AZ II), the most abundant benthic foraminifers are represented by alveolinids, miliolids, coskinolinids, and subordinate rotaliids. The presence of miliolids, along with agglutinated foraminifers (coskinolinids) can be assigned to a proximal inner ramp setting (Vecchio & Hottinger, 2007). Moreover, the occurrence of alveolinids, miliolids, and coskinolinids may be developed from the distal inner ramp to the middle ramp.

In nummulitids-discocyclinids Assemblage Zone (AZ III), the orthophragminids (*Discocyclina*) have been described from a wide range of environments within the shallow marine (*e.g*., back and fore reef/shoal) (Ghose, 1977) to deeper settings (*e.g*., outer shelf/ramp) (Buxton & Pedley, 1989; Eichenseer & Luterbacher 1992; Beavington-Penney & Racey, 2004). The small and robust *Nummulites* Lamarck, 1801 were spread throughout the Tethyan region from the eastern Alps to the Middle East (eastern Iran) and occurred in a broad range of open marine environments during the Eocene, whereas they are found within the inner ramp during the Paleocene (Rasser *et al*., 1999; Romero *et al*., 2002; Nebelsick *et al*., 2005). The co-occurrence of small *Nummulites* and *Discocyclina* Gumbel, 1870 suggests shallow depth inner and middle ramp settings. On the other hand, the planktonic foraminifers prefer to be present in a calm, low-energy environment and the deep environment with dominant normal salinity water and reduced light intensity. Therefore, these three associations extend from the inner ramp setting to the proximal outer ramp depositional environment.

CONCLUSIONS

Three foraminiferal assemblages are presented in the Mahallat region for the first time. Two of them match well with SBZ 11 and SBZ 12 of the Standard Shallow Benthic Zones of Serra-Kiel *et al*. (1998) and BouDagher-Fadel *et al*. (2015).

In the Assemblage Zone I, there are three index foraminifers: *Assilina laxispira*, *Granorotalia sublobata* and *Decrouezina aegyptiaca* (Figure 10). The *G. sublobata* can be the best marker of the SBZ 11 of Standard Shallow Benthic Zones of Serra-Kiel *et al*. (1998).

The three new species *Daviesiconus mahallatensis* sp. nov., *Barattolites arghadehensis* sp. nov., and *Coleiconus minimus* sp. nov. are identified in the Assemblage Zone II and described for the first time. The first two species occur in the middle–late Cuisian and the third species is only found in the late Cuisian. The co-occurrence of the alveolinid species (Figure 10) with the newly recorded taxa of agglutinated foraminifers indicates a middle–late Cuisian age (SBZ 11-12). Therefore, the three new taxa can be used for establishing at least a regional biostratigraphy of the Cuisian strata. They can be correlated with the simultaneous taxa. Therefore, the systematic description and the stratigraphic distribution of the three new species, along with the marker foraminifers are the purposes of this article.

The planktonic foraminifers presented in the Assemblage Zone III are considered marker fossils, but the benthic foraminifers have never been an indicator for the biostratigraphic scheme. In this work, due to the stratigraphic location and the concurrent range of the recorded planktonic foraminifers, the biostratigraphic range of this zone is attributed to the Lutetian stage.

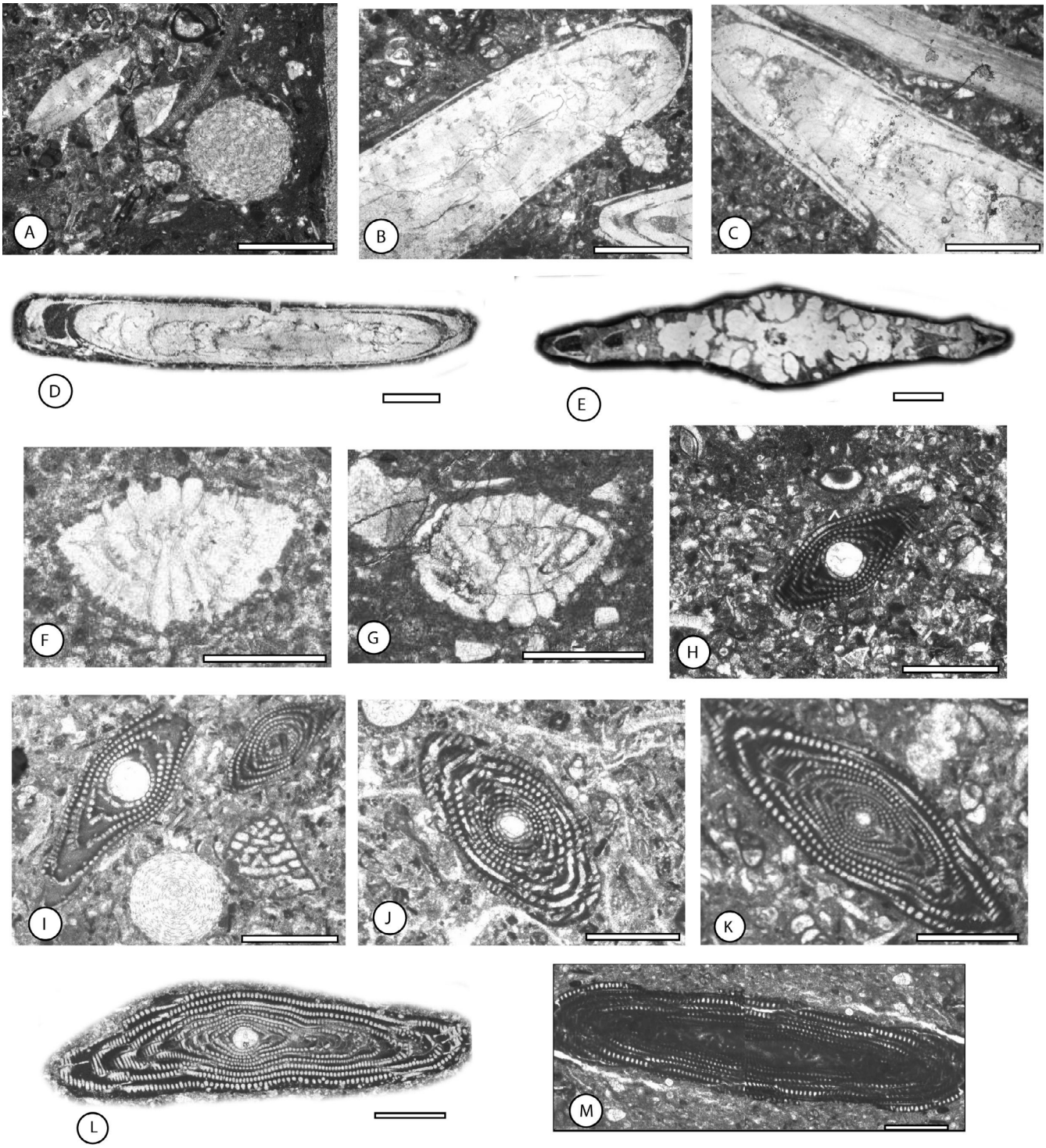

Figure 10. Photographs of foraminiferal species. **A**, *Sphaerogypsina globulus*, equatorial section, thin section 213; **B**–**C**, *Assilina laxispira*, subaxial section, thin section 203; **D**, *Assilina laxispira*, axial section, thin section 203, **E**, *Decrouezina aegyptiaca*, axial section, thin section 207; **F**, *Granorotalia sublobata*, axial section, thin section 209; **G**, *Granorotalia* cf. *sublobata*, subaxial section, thin section 206; **H**, *Alveolina cremae*, axial section, thin section 233; **I**, *Alveolina cremae*, axial section, *Sphaerogypsina globulus*, equatorial section, thin section 237; **J**, *Alveolina decastroi*, axial section, thin section 225; **K**, *Alveolina distefanoi*, axial section, thin section 225; **L**, *Alveolina levantina*, axial section, thin section 211; **M**, *Alveolina frumentiformis*, subaxial section, thin section 240. Scale bars: A–E, H–M = 1 mm; F–G = 0.5 mm.

ACKNOWLEDGEMENTS

I greatly acknowledge the facilities provided by the Department of Geology of Payame Noor University. I also thank A. Benedetti for constructive comments on some hyaline foraminifera (rotalids). Text editing by D. Cluzel is kindly acknowledged. I also thank M. Beiki for their generous help during fieldwork. The manuscript benefits from the final edition of the editor.

REFERENCES

Accordi, G.; Carbone, F. & Pignatti, J. 1998. Depositional history of a Paleogene carbonate ramp (Western Cephalonia, Ionian Islands, Greece). *Geologica Romana*, **34**:131–205.

Afzal, J.; Williams, M.; Leng, M.J.; Aldridge, R.J. & Stephenson, M.H. 2011. Evolution of Paleocene to Early Eocene larger benthic foraminifer assemblages of the Indus Basin, Pakistan. *Lethaia*, **44**:299–320. *doi:10.1111/j.1502-3931.2010.00247.x*

Babazadeh, S.A. 2008. Lower Eocene transgressive successions of Sahlabad province, eastern Iran, implication of biostratigraphy and microfacies analysis. *Revue de Paleobiologie*, **27**:449–459.

Beavington-Penney, S.J. & Racey, A. 2004. Ecology of extant nummulitids and other larger benthic foraminifera: applications in paleoenvironmental analysis. *International Journal Herat Sciences*, **67**:219–265.

Benedetti, A.; Di Carlo, M. & Pignatti, J. 2011. New Late Ypresian (Cuisian) Rotaliids (Foraminiferida) from Central and Southern Italy and their Biostratigraphic Potential. *Turkish Journal of Earth Sciences*, **20**:701–719.

Berggren, W.A.; Pearson, P.N.; Huber, B.T. & Wade, B.S. 2006. Taxonomy, biostratigraphy, and phylogeny of Eocene *Acarinina*. *Cushman Foundation special publication*, **41**:257–326.

BouDagher-Fadel, M.K.; Price, G.D.; Hu, X. & Li, J. 2015. Late Cretaceous to early Paleogene foraminiferal biozones in the Tibetan Himalayas, and a pan-Tethyan foraminiferal correlation scheme. *Stratigraphy*, **12**:67–91.

Buxton, M.W.N. & Pedley, H.M. 1989. A standardized model for Tethyan Tertiary carbonate ramp. *Journal of Geology Society*, **146**:746–748. *doi:10.1144/gsjgs.146.5.074*

Cole, W.S. 1942. Stratigraphic and paleontologic studies of wells in Florida. *Bulletin Florida Geology Survey*, **20**:1–89.

Davies, L.M. 1930. The genus *Dictyoconus* and its allies: review of the group, together with a description of three new species from the Lower Eocene beds of northern Baluchistan. *Transactions of the Royal Society of Edinburgh*, **56**:485–505.

Drobne, K. 1977. Alveolines palèogenes de la Slovenie et de l'Istrie. *Schweizerische Paläontologische Abhandlungen*, **99**:1–132.

Drobne, K.; Ćosovic, V.; Moro, A. & Buckovic D. 2011. The role of the Paleogene Adriatic carbonate platform in the spatial distribution of Alveolinids. *Turkish Journal of Earth Sciences*, **20**:721–751.

Eichenseer, H. & Luterbacher, H.P. 1992. The marine Paleogene of the Tremp region (NE Spain). Depositional sequences, facies history, biostratigraphy and controlling factors. *Facies*, **27**:119–152. *doi:10.1007/BF02536808*

Geel, T. 2000. Recognition of stratigraphic sequences in carbonate platform and slope deposits, empirical model based on microfacies analysis of Paleogene deposits in southeastern Spain. *Palaeogeography*, *Palaeoclimatology*, *Palaeoecology*, **155**:211–238. *doi:10.1016/S0031-0182(99)00117-0*

Ghose, B.K. 1977. Paleoecology of the Cenozoic reefal foraminifers and algae-a brief review. *Palaeogeography*, *Palaeoclimatology*, *Palaeoecology*, **22**:231–256. *doi:10.1016/0031-0182(77)90030-X*

Hayward, B.W.; Le Coze, F.; Vachard, D. & Gross, O. 2022**.** World foraminifera database. Available at https://www.marinespecies.org/foraminifera; accessed on 10/21. *doi:10.14284/305*

Henson, F.R.S. 1948. *Larger imperforate foraminifera of south-western Asia. Families Lituolidae*, *Orbitolinidae and Meandropsinidae*. London, S.W., British Museum (Natural History), 127 p.

Hottinger, L. 1960. Recherches sur les Alveolins du Paléocène et de l'Eocène. *Mémoires Suisses de Paléontologie*, **75–76**:1–243.

Hottinger, L. 2007. Revision of the foraminiferal genus *Globoreticulina* Rahaghi, 1978, and of its associated fauna of larger foraminifera from the late Middle Eocene of Iran. *Carnets de Géologie*, 1–51.

Hottinger, L. & Drobne, K. 1980. Early Tertiary conical imperforate foraminifera. *Razprave Slov Akad Znan Umet*, **22**:187–276.

Kaminski, M.A. 2004. The year 2000 classification of the agglutinated foraminifera. *Grzybowski Foundation Special Publication*, **8**:237–255.

Kaminski, M.A. 2014. The year 2010 classification of the agglutinated foraminifera. *Micropaleontology*, **60**:89–108.

Luterbacher, H. 1984. Paleoecology of foraminifera in the Paleogene of the southern Pyrenees. *Bulletin Centre de Recherches Exploration-Production Elf-Aquitaine Memoire*, **6**:389–392.

Nafarieh, E.; Boix, C.; Cruz-Abad, E.; Ghasemi-Nejad, E.; Tahmasbi, A. & Caus, E. 2019. Imperforate larger benthic foraminifera from shallow-water carbonate facies (Middle and Late Eocene), Zagros Mountains, Iran. *Journal of Foraminiferal Research*, **49**:275–302. *doi:10.2113/gsjfr.49.3.275*

Nebelsick, J.H.; Rasser, M.W. & Bassi, D. 2005. Facies dynamics in Eocene to Oligocene circumalpine carbonates. *Facies*, **51**:197–216. *doi:10.1007/s10347-005-0069-2*

Ozgen-Erdrem, N.; Inan, N.; Akyazi, M. & Tunoglu, C. 2005. Benthic foraminifera assemblages and microfacies analysis of Paleocene-Eocene carbonate rocks in the Kastamonu region, Northern Turkey. *Journal of Asian Earth Sciences*, **25**:405–422. *doi:10.1016/j.jseaes.2004.04.005*

Racey, A. 1994. Biostratigraphy and paleobiogeographic significance of Tertiary nummulitids (foraminifera) from northern Oman. *In:* M.D. Simmons (ed.) *Micropaleontology and hydrocarbon exploration in the Middle-East*, Springer, p. 309–312.

Rahaghi, A. 1980. Tertiary faunal assemblage of Qom-Kashan, Sabzewar and Jahrum area. Tehran. *National Iranian Oil Company*, **8**:1–126.

Rahaghi, A. 1983. Stratigraphy and faunal assemblage of Paleocene and Lower Eocene in Iran. *National Iranian Oil Company*, **10**: 1–173.

Rahaghi, A. & Schaub, H. 1976. *Nummulites* et *Assilines* du N.E. de l'Iran. *Eclogae Geologicae Helvetiae*, **69**:765–782.

Rasser, M.W.; Scheibner, C. & Mutti, M. 2005. A paleoenvironmental standard section for Early Ilerdian tropical carbonate factories (Corbieres, France: Pyrenees, Spain). *Facies*, **51**:217–232.

Romero, J.E.; Caus, E. & Rosell, J. 2002. A model for the palaeoenvironmental distribution of larger foraminifera based on late Middle Eocene deposits on the margin of the South Pyrenean basin (NE Spain). *Palaeogeography*, *Palaeoclimatology*, *Palaeoecology*, **179**:43–56.

Samuel, K.; Borza, E. & Kohler, E. 1972. *Microfauna and lithostratigraphy of the Paleogene and adjacent Cretaceous of the*

middle Vah Valley (west Carpatian). Bratislava, Geologický ústav Dionýza Stúra, 246 p.

Saraswati, P.K.; Patra, P.K. & Banerji, R.K. 2000. Biometric study of some Eocene *Nummulites* and *Assilina* from Kutch and Jaisalmer, India. *Journal of the Palaeontological Society of India*, **45**:91–122.

Saraswati, P.K.; Sarkar, U. & Banerjee, S. 2012. *Nummulites solitarius – Nummulites burdigalensis* lineage in Kutch with Remarks on the Age of Naredi Formation. *Journal of the Geological Society of India*, **79**:476–482.

Schaub, H. 1966. Ueber die Grossforaminiferen im Untereocaen von Campo (Ober-Aragonien). *Eclogae Geologicae Helvetiae*, **59**:355–377.

Schaub, H. 1973. La seccion de Campo (provincia de Huesca). *In*: EUROPEAN MICROPALAEONTOLOGICAL COLLOQUIUM, 13, 1973. *Livret-guide*, p. 151–170.

Schaub, H. 1981. Nummulites et Assilines de la Tethys paleogène. Taxonomie, phylogènese, biostratigraphie. *Memoires Suisses de Paleontologie*, **104–106**:1–236.

Scheibner, C.; Rasser, M.W. & Mutti, M. 2007. The Campo section (Pyrenees, Spain) revised: Implications for changing carbonate assemblages across the Paleocene-Eocene boundary. *Palaeogeography*, *Palaeoclimatology*, *Palaeoecology*, **248**:145–168. *doi:10.1016/j.palaeo.2006.12.007*

Scheibner, C. & Speijer, R.P. 2008. Decline of coral reefs during late Paleocene to early Eocene global warming, *eEarth*, **3**:19–26. *doi:10.5194/ee-3-19-2008*

Scheibner, C.; Speijer, R.P. & Marzouk, A.M. 2005. Larger foraminiferal turnover during the Paleocene/Eocene Thermal Maximum and paleoclimatic control on the evolution of platform ecosystems. *Geology*, **33**:493–496. *doi:10.1130/G21237.1*

Serra-Kiel, J.S.; Gallardo-Garcia, A.; Razin, P.; Robinet, J.; Roger, J.; Grelaud, C.; Leroy, S. & Robin, C. 2016. Middle Eocene–Early Miocene larger foraminifera from Dhofar (Oman) and Socotra Island (Yemen). *Arabian Journal of Geosciences*, p. 1–95.

Serra-Kiel, J.S. *et al*. 1998. Larger foraminiferal biostratigraphy of the Tethyan Palaeocene and Eocene. *Bulletin de la Société Géologique de France*, **169**:281–299.

Sheikholeslami, M.R. 2005. Geological map of Mahallat, Project coordinate system, WGS 1984. Geological Survey of Iran.

Silvestri, A. 1939: Foraminiferi del1 Eocene della Somalia II. *Palaeontografia italica*, **32**:1–102.

Vecchio, E. 2003. *La "Facies a Spirolina" nelle successioni carbonatiche del Paleocene-Eocene dell'Italia Meridionale: paleontologia*, *paleoecologia e biostratigrafia delle associazioni a foraminiferi bentonici*, Università degli Studi di Napoli Federico, Ph.D. Thesis, 171 p.

Vecchio, E. & Hottinger, L. 2007. Agglutinated conical foraminifera from the Lower–Middle Eocene of the Trentinara Formation (southern Italy): *Facies*, **53**:509–533. *doi:10.1007/s10347-007-0112-6*

Zamagni, J.; Mutti, M. & Kosir, A. 2008. Evolution of shallow benthic communities during the Late Paleocene- Earliest Eocene transition in the Northern Tethys (SW Slovenia). *Facies*, **54**:25–43. *doi:10.1007/s10347-007-0123-3*

Zhang, Q.; Willems, H. & Ding, L. 2013. Evolution of the Paleocene-Early Eocene larger benthic foraminifera in the Tethyan Himalaya of Tibet, China. *International Journal of Earth Sciences*, **102**:1427–1445. *doi:10.1007/s00531-012-0856-2*

Received in 05 August, 2022; accepted in 11 November, 2022.